



Chinese Pharmaceutical Association
Institute of Materia Medica, Chinese Academy of Medical Sciences

Acta Pharmaceutica Sinica B

www.elsevier.com/locate/apsb
www.sciencedirect.com



ORIGINAL ARTICLE

Bacteroides fragilis-derived succinic acid promotes the degradation of uric acid by inhibiting hepatic AMPD2: Insight into how plant-based berberine ameliorates hyperuricemia



Libin Pan^{a,†}, Ru Feng^{a,†}, Jiachun Hu^{a,†}, Hang Yu^a, Qian Tong^b, Xinyu Yang^{a,b}, Jianye Song^a, Hui Xu^a, Mengliang Ye^a, Zhengwei Zhang^a, Jie Fu^a, Haojian Zhang^a, Jinyue Lu^a, Zhao Zhai^a, Jingyue Wang^{a,b}, Yi Zhao^a, Hengtong Zuo^a, Xiang Hui^a, Jiandong Jiang^{a,*}, Yan Wang^{a,*}

^aState Key Laboratory of Bioactive Substance and Function of Natural Medicines, Institute of Materia Medica, Chinese Academy of Medical Sciences/Peking Union Medical College, Beijing 100050, China

^bThe First Hospital of Jilin University, Changchun 130021, China

Received 23 November 2024; received in revised form 13 June 2025; accepted 26 June 2025

KEY WORDS

Berberine;
Hyperuricemia;
Gut microbiota;
AMPD2;
Succinic acid;
Uric acid synthesis;
Gut–liver axis;
Bacteroides fragilis

Abstract In recent decades, the prevalence of hyperuricemia and gout has increased dramatically due to lifestyle changes. The drugs currently recommended for hyperuricemia are associated with adverse reactions that limit their clinical use. In this study, we report that berberine (BBR) is an effective drug candidate for the treatment of hyperuricemia, with its mechanism potentially involving the modulation of gut microbiota and its metabolite, succinic acid. BBR has demonstrated good therapeutic effects in both acute and chronic animal models of hyperuricemia. In a clinical trial, oral administration of BBR for 6 months reduced blood uric acid levels in 22 participants by modulating the gut microbiota, which led to an increase in the abundance of *Bacteroides* and a decrease in *Clostridium sensu stricto_1*. Furthermore, *Bacteroides fragilis* was transplanted into ICR mice, and the results showed that *Bacteroides fragilis* exerted a therapeutic effect on uric acid similar to that of BBR. Notably, succinic acid, a metabolite

*Corresponding authors.

E-mail addresses: wangyan@imm.ac.cn (Yan Wang), jiang.jdong@163.com (Jiandong Jiang).

[†]These authors made equal contributions to this work.

Peer review under the responsibility of Chinese Pharmaceutical Association and Institute of Materia Medica, Chinese Academy of Medical Sciences.

<https://doi.org/10.1016/j.apsb.2025.08.009>

2211-3835 © 2025 The Authors. Published by Elsevier B.V. on behalf of Chinese Pharmaceutical Association and Institute of Materia Medica, Chinese Academy of Medical Sciences. This is an open access article under the CC BY-NC-ND license (<http://creativecommons.org/licenses/by-nc-nd/4.0/>).

of *Bacteroides*, significantly reduced uric acid levels. Subsequent cell and animal experiments revealed that the intestinal metabolite, succinic acid, regulated the upstream uric acid synthesis pathway in the liver by inhibiting adenosine monophosphate deaminase 2 (AMPD2), an enzyme responsible for converting adenosine monophosphate (AMP) to inosine monophosphate (IMP). This inhibition resulted in a decrease in IMP levels and an increase in phosphate levels. The reduction in IMP led to a decreased downstream production of hypoxanthine, xanthine, and uric acid. BBR also demonstrated excellent renoprotective effects, improving nephropathy associated with hyperuricemia. In summary, BBR has the potential to be an effective treatment for hyperuricemia through the gut–liver axis.

© 2025 The Authors. Published by Elsevier B.V. on behalf of Chinese Pharmaceutical Association and Institute of Materia Medica, Chinese Academy of Medical Sciences. This is an open access article under the CC BY-NC-ND license (<http://creativecommons.org/licenses/by-nc-nd/4.0/>).

1. Introduction

An increase in the prevalence of hyperuricemia has been noted due to the intake of high-energy diets (high in sugar, fat, and protein) over the past decades, and the age of hyperuricemia onset is becoming younger¹. Hyperuricemia has become the second most common metabolic disease in China after diabetes². Hyperuricemia is defined as a serum uric acid concentration >7 mg/dL (>420 μmol/L) in males and >6 mg/dL (>360 μmol/L) in females. Uric acid is mainly synthesized in the liver and is the end product of the metabolism of nucleosides in food and a precursor for substances involved in nucleotide synthesis and endogenous purine metabolism (including DNA decomposition products and adenosine triphosphate (ATP) decomposition products). Hyperuricemia often occurs with complications, among which gout arthritis is the most common³. Approximately 2/3 of uric acid elimination occurs in the urine through the kidney, and the rest is excreted in the gastrointestinal tract⁴. Both the overproduction and reduced excretion of uric acid can lead to hyperuricemia. For instance, the knockdown of uric acid transporters glucose transporters 9 and ATP-binding cassette transporter G2 in the gut results in hyperuricemia⁵. Long-term high plasma uric acid levels often lead to renal impairment and worse renal pathology, including segmental glomerulosclerosis, tubular atrophy, and interstitial fibrosis⁶. At present, the mechanisms of the drugs for hyperuricemia are mainly as follows: 1) inhibition of xanthine oxidase; 2) promotion of the renal excretion of uric acid; and 3) the use of recombinant uricase to oxidize uric acid to produce allantoin. Nevertheless, xanthine oxidase inhibitors remain the mainstream drugs used to reduce blood uric acid in the clinic, but serious side effects and poor patient compliance hamper their clinical use⁷.

Recent studies have shown that febuxostat, a xanthine oxidase inhibitor, may be associated with an increased incidence of all-cause mortality and cardiovascular disease⁷. Uric acid excretion drugs increase the risk of inducing kidney stones and have contraindications, including impaired renal function and chronic liver disease. Recombinant uricase (uric acid oxidase) can generate allantoin by oxidizing uric acid, thereby reducing the level of uric acid content, and is mainly used to treat refractory gout when the abovementioned drugs are ineffective; however, its large-scale use is limited due to its drug immunogenicity. Therefore, finding and developing safe and effective drugs to alleviate hyperuricemia is very important.

Recent studies suggest that the gut microbiota plays a major role in hyperuricemia and gout. Patients with hyperuricemia often experience changes in the structure and function of the intestinal

flora^{8,9}. Moreover, the gut microbiota participates in the metabolism of uric acid precursors and decomposes uric acid to influence the level of uric acid precursors and uric acid entering the circulatory system¹⁰. Metabolites produced by the intestinal flora affect the excretion of uric acid¹¹. The gut microbiota is also involved in the regulation of immune inflammation in patients with gout¹². However, the specific intestinal flora and their metabolism of uric acid are still unclear and are worthy of in-depth study.

Berberine (BBR) is the main active ingredient of the traditional Chinese medicine *Coptis chinensis* Franch. The safety and efficacy of BBR, as a common natural medicine for diarrhea, have been demonstrated throughout the years of usage. Moreover, the low solubility and poor permeability (ionic form) of BBR result in low bioavailability, which leads to the accumulation of a large amount of BBR in the gut and provides the possibility of interactions between BBR and the gut microbiota; thus, studies on the therapeutic efficacy and mechanism of BBR *via* the gut microbiota have emerged, including studies on hyperlipidemia^{13,14}, type 2 diabetes¹⁵, chronic kidney disease¹⁶, Parkinson's disease¹⁷, and nonalcoholic fatty liver disease¹⁸. BBR could be a promising candidate drug for the treatment of energy metabolism disorders *via* a multitarget mechanism.

In this study, we revealed the therapeutic effect of BBR in hyperuricemia *via* the gut–liver axis. BBR significantly alleviated hyperuricemia and the gut microbiota disturbances caused by hyperuricemia. In particular, BBR restored the abundance of *Bacteroides* and reduced the abundance of *Clostridium sensu stricto_1* in both animal models and clinical fecal samples. *Bacteroides fragilis* transplantation experiments revealed that *B. fragilis* significantly decreased blood uric acid levels and increased the content of succinic acid, which altered uric acid metabolism in the liver. Furthermore, BBR directly inhibited the activity of AMPD2 to reduce the production of uric acid in the liver, suggesting that this natural drug may have the potential to regulate nucleic acid metabolism in addition to regulating glycolipid metabolism^{13,15}.

2. Materials and methods

2.1. Cell culture

Human embryonic kidney 293T (HEK293T) cells (China Infrastructure of Cell Line Resource, Beijing, China) were cultured in Dulbecco's modified Eagle's medium (Gibco, Thermo Fisher Scientific, Inc., Waltham, MA, USA) supplemented with 10% fetal bovine serum (Gibco, Thermo Fisher Scientific, Inc.) and 1% penicillin–streptomycin (Jiangsu KeyGEN BioTECH Co., Ltd.,

Nanjing, China). HEK293T cells were cultured in an incubator at 37 °C with 95% humidity and 5% CO₂, respectively.

Bacteroides fragilis (ATCC 25285) was cultured in *Bacteroides* Phage Recovery Medium Broth (Psaitong Co., Ltd., China) supplemented with 5% fetal bovine serum (Gibco, Thermo Fisher Scientific, Inc.) at 37 °C under anaerobic conditions.

2.2. Pharmacodynamic study of BBR in ICR mice with chronic hyperuricemia

Forty 8-week-old male ICR mice were randomly divided into four groups: the control group, the model group, the BBR low-dose group (BBR, 100 mg/kg) and the BBR high-dose group (BBR, 200 mg/kg). After one week of adaptive feeding, the model was established by administering a high-purine diet (10% yeast powder) and intraperitoneally injecting potassium oxazinate (100 mg/kg/day). After 4 weeks of modeling, the mice in the BBR low-dose group and the BBR high-dose group were given BBR (orally, 100 mg/kg/day or 200 mg/kg/day) while continuing modeling; subsequently, blood samples were taken to determine the levels of plasma uric acid 1 week and 2 weeks after drug administration. At the end of the experiment, fecal samples were collected for analysis of the gut microbiota composition. The V3 and V4 regions were analyzed by 16S rRNA gene sequencing (See [Supporting Information](#)).

2.3. Pharmacodynamic study of BBR in ICR mice with acute hyperuricemia

Fifty 8-week-old male ICR mice were randomly divided into 5 groups, namely, the control group (Control Group), the model group (Model Group), the BBR low-dose group (BBR-L, 100 mg/kg), the BBR high-dose group (BBR-H, 200 mg/kg) and the positive group (benzbromarone, 20 mg/kg). After one week of adaptive feeding, the model was established by 2 weeks of continuous oral administration of xanthine (50 mg/kg/day) and intraperitoneal injection of potassium oxazinate (100 mg/kg/day). Drug administration was performed while modeling. After two weeks of intervention, blood samples were collected, and uric acid and creatinine levels in the blood were measured using the corresponding detection kits. The animal experiment was conducted in strict accordance with the guidelines and ethical guidelines for experimental animals and was approved by the Animal Ethics Committee of the Institute of Experimental Zoology of the Chinese Academy of Medical Sciences and Peking Union Medical College (No. 00003464, 00003546, 00002648).

2.4. Determination of the levels of metabolites in the AMPD2 metabolic pathway using LC-MS/MS

The quantitative determination of uric acid, xanthine, hypoxanthine, inosine, AMP, and IMP levels was performed by high-performance liquid chromatography–triple quadrupole mass spectrometry (LCMS-8060, Shimadzu, Kyoto, Japan). An Alltima C18 (5 µm, 4.6 mm × 150 mm) column was used for chromatographic separation. The linear gradient elution flow rate was 0.4 mL/min. Water was used as mobile phase A, and methanol was used as mobile phase B. The gradient elution procedure was as follows: 1.00 min (95% A and 5% B), 14.00 min (10% A and 90% B), 17.00 min (10% A and 90% B), 17.01 min (95% A and 5% B), and stopping at 22 min. The column temperature was

maintained at 40 °C. The detection method used for mass spectrometry was multiple reaction mode (MRM). The mass spectrometry parameters were set as follows: 1) nebulizing gas flow, 2.8 L/min; 2) heating gas flow, 10.0 L/min; 3) drying gas flow, 10.0 L/min; 4) interface temperature, 300 °C; 5) DL temperature, 250 °C; and 6) heating block temperature, 400 °C. The *m/z* transitions are 167.15 → 124.00 (*m/z*) for uric acid, 135.40 → 92.05 (*m/z*) for hypoxanthine, 151.35 → 108.05 (*m/z*) for xanthine, 267.25 → 135.10 (*m/z*) for inosine, 346.25 → 79.05 (*m/z*) for AMP, 347.25 → 79.00 (*m/z*) for IMP.

Plasma was collected by centrifuging the blood samples at 3380 × *g* for 5 min at 4 °C. Then, 3 times the volume of acetonitrile (including IS) was added to 50 µL of plasma for protein precipitation. After centrifugation at 13,500 × *g* for 5 min, 5 µL of the supernatant was collected for analysis.

2.5. Clinical study of the efficacy of BBR in ameliorating hyperuricemia

Eight hyperuricemia patients (2 males, 6 females; age 68.75 ± 4.65 with high levels of blood uric acid: 421.6 ± 57.52 mmol/L) and 14 volunteers without hyperuricemia (9 males, 5 females; age 63.00 ± 5.68 with normal levels of blood uric acid: 320.0 ± 65.52 mmol/L) were enrolled in this study in the Outpatient Section of the First Hospital of Jilin University in Changchun in the summer of 2017. This study was approved by the institutional ethics committee of the First Hospital of Jilin University (ChiCTR-OPN-17012942), and all patients and volunteers without hyperuricemia signed informed consent forms. Notably, the abovementioned study was a subgroup analysis of a clinical study in patients with abnormal lipid metabolism and atherosclerosis, so all subjects received BBR (0.5 g, bid, for 6 months) for intervention. In this part of the study, we focused mainly on the blood uric acid index and the renal function index.

The criteria for hyperuricemia were as follows: under normal diet conditions, after fasting for more than 12 h before the test, fasting blood uric acid levels >420 µmol/L for males and >360 µmol/L for females on two different days.

The 22 enrolled volunteers were orally administered BBR (0.5 g, bid) for 6 months. Blood samples were collected in the morning on the first day and 2, 4 and 6 months later and stored at −20 °C. Blood uric acid, serum creatinine and blood urea nitrogen (BUN) levels were measured by the Laboratory Department of the First Hospital of Jilin University using a Hitachi series 7600 automatic biochemical analyzer (Tokyo, Japan). At the same time, fecal samples were collected for analysis of the gut microbiota composition.

2.6. Correlation analysis of the uric acid content in serum and the intestinal flora in patients with hyperuricemia

Feces were collected before treatment and 2, 4, and 6 months after BBR treatment. The V3 and V4 regions were analyzed by 16S rRNA gene sequencing. The correlations between microbiota at the genus level and plasma uric acid content were evaluated.

2.7. The hypouricemic effect of *Bacteroides fragilis* in animals with fructose-induced hyperuricemia

Thirty-six eight-week-old male ICR mice were randomly divided into 4 groups: the control group (*n* = 9), the model group (*n* = 9),

the *Bacteroides fragilis* group ($n = 9$) and the combined treatment group (*Bacteroides fragilis* and BBR, $n = 9$). The model group, the *Bacteroides fragilis* group, and the combined treatment group were fed 10% fructose in the drinking water and were intraperitoneally injected with 100 mg/kg/day potassium oxazinate (2 times a day, at 8:00 and 18:00) for 7 consecutive days. The exposure conditions of each group were as follows: 1) the *Bacteroides fragilis* group was orally administered 1×10^{10} colony-forming units (CFUs) of *Bacteroides fragilis* per day, and 2) the combined treatment group was treated with 1×10^{10} CFUs of *Bacteroides fragilis* per day and orally administered BBR (200 mg/kg). Plasma was collected after 7 days of treatment, and the uric acid level was determined by LC-MS/MS. Fecal samples were collected for the determination of short-chain fatty acid levels.

2.8. Determination of short-chain fatty acid levels in vitro

Fecal samples (approximately 0.2 g) from the previous experiment were pretreated by dilution [weight (g): volume (μL) = 1:1000] in water. The mixture was centrifuged at $18,400 \times g$ for 10 min at 4°C . Then, 100 μL of the supernatant was added to acetone (with 1% phosphoric acid, v/v) for short-chain fatty acid (SCFA) extraction. The mixture was centrifuged at $18,400 \times g$ for 10 min at 4°C , and the supernatant was directly injected for analysis. The quantification of SCFAs by gas chromatography (GC) was performed as previously described¹⁹. A gas chromatograph (GC-2020) from Shimadzu Corporation (Kyoto, Japan) was used in this study. A high polarity Alltech capillary column (AT-WAX, $30 \text{ m} \times 0.25 \text{ mm} \times 0.25 \mu\text{m}$, Alltech Corporation, Chicago, USA) was used for separation with the following parameters: nitrogen flow, 1.27 mL/min; purge flow, 3.0 mL/min; total pressure, 105.0 kPa; injection port temperature, 230°C ; and FID detector temperature, 250°C . The temperature program started at 80°C for 1 min, linearly increased to 130°C at a rate of $5^\circ\text{C}/\text{min}$, and was maintained for 5 min.

2.9. The hypouricemic effect of sodium succinate in animals with hyperuricemia

Forty 8-week-old male C57BL/6 mice were randomly divided into 5 groups, namely, the control group, the model group, the BBR group (200 mg/kg), the SUC group (sodium succinate, 200 mg/kg), and the positive control group (benzbromarone, 20 mg/kg). After one week of adaptive feeding, the model was continuously established for 30 days via 300 mmol/L sodium glutamate (final concentration) in the drinking water. Drug administration was performed during modeling. After 30 days, orbital blood samples and the liver were collected for further study.

Forty 8-week-old male ICR mice were randomly divided into 5 groups: the control group, the model group, the BBR group (200 mg/kg), the SUC group (sodium succinate, 200 mg/kg), and the positive control group (benzbromarone, 20 mg/kg). The model was continuously established by feeding with 10% fructose in the drinking water, as well as injecting potassium oxazinate intraperitoneally (100 mg/kg/day, 2 times a day, at 8:00 and 18:00) for 7 consecutive days. After 7 days of intervention, orbital blood samples and the liver were collected for further study.

The levels of metabolites in the AMPD2 metabolic pathway in plasma were determined by LC-MS/MS. The levels of uric acid, BUN, and creatinine were determined by the corresponding test kits. The phosphate level and enzyme activity of AMPD2 in the liver were evaluated as described above.

2.10. Effect of succinic acid on the purine metabolism pathway in HEK293T cells

To test the effect of succinic acid on normal HEK293T cells viability, HEK293T cell lines were purchased from Beijing Hexiucheng Biotechnology Co., Ltd. (Beijing, China). Routine culture was performed in DMEM supplemented with 100 units/mL penicillin and 100 mg/mL streptomycin and 10% fetal bovine serum at 37°C and 5% CO_2 incubation condition.

HEK293T cells were cultured in 96-well plates for 24 h until the cells were adherent. Succinic acid of 10 mmol/L, 5 mmol/L, 2.5 mmol/L, 1.25 mmol/L, 625 $\mu\text{mol/L}$, 312.5 $\mu\text{mol/L}$ and 156.25 $\mu\text{mol/L}$ were added to the plates, respectively. After 24 h of culture in the incubator, the cell viability was measured by CCK8 kit (Solarbio, Beijing, China).

Then, the effect of succinic acid on purine metabolism pathway in normal HEK293T cells was carried out. HEK293T cells were cultured in 12-well plates for 24 h until the cells were adherent. DMSO, 2.5 mmol/L, 1.25 mmol/L and 625 $\mu\text{mol/L}$ succinic acid were added to the cells, respectively, and cultured in an incubator for 24 h. Phosphate and ATP were determined using the phosphate detection kit and ATP detection kit (Beyotime, Shanghai, China). AMP, IMP, inosine, hypoxanthine, xanthine, and uric acid were determined using LCMS-8060.

Finally, fructose-induced HEK293T cells were used to test the effects of succinic acid on purine metabolism pathway. HEK293T cells were cultured in a 12-well plate and cultured for 24 h until the cells were adherent. DMSO, fructose (20 mmol/L), fructose (20 mmol/L) + 625 $\mu\text{mol/L}$ succinic acid (SA-L) and fructose (20 mmol/L) + 2.5 mmol/L succinic acid (SA-H) were added to the plates, respectively. After 24 h of continuous culture, the phosphate detection kit and ATP detection kit (Beyotime, Shanghai, China) were used for determination.

2.11. Effect of BBR on nephropathy in animals with hyperuricemia

Thirty-five 8-week-old male SD rats were randomly divided into 5 groups, namely, the control group (control group), the model group (model group), the positive control group (febuxostat, 10 mg/kg/day), the BBR low-dose group (BBR, 100 mg/kg/day) and the BBR high-dose group (BBR, 200 mg/kg/day). After one week of adaptive feeding, the model was established by feeding the animals 10% yeast with 0.15% adenine continuously for 6 weeks. Drug intervention was conducted during modeling. After 6 weeks of intervention, the levels of xanthine, uric acid, creatinine, and trimethylamine-*N*-oxide (TMAO) in plasma were determined by using LC-MS/MS, while the level of BUN was determined by a BUN assay kit from Nanjing Jiancheng Institute of Bioengineering (Nanjing, China). Kidneys were fixed with 4% paraformaldehyde (Beijing Solarbio Technology Co., Ltd., Beijing, China), embedded in conventional paraffin, sliced and stained with an HE staining kit (Beijing Solarbio Technology Co., Ltd., Beijing, China).

2.12. Statistical analysis

The data were analyzed using Prism version 8.0 (GraphPad Software, La Jolla, CA, USA). The data in the figures are expressed as the mean \pm standard deviation (SD), and the differences between groups were analyzed by a two-sided *t* test. *P* values less than 0.05 were considered to indicate statistical

significance ($*P < 0.05$, $**P < 0.01$, and $***P < 0.001$). A P value less than 0.05 is considered statistically significant.

3. Results

3.1. BBR significantly improves chronic/acute hyperuricemia in ICR mice

First, we established a chronic hyperuricemia model with ICR mice by feeding them a high-purine diet and injecting potassium oxazinate intraperitoneally to investigate the therapeutic effect of BBR on hyperuricemia (Fig. 1A). After 6 weeks of modeling, the plasma uric acid concentration in the model group was significantly greater than that in the control group ($***P < 0.001$), indicating that the hyperuricemia model was successfully established (Fig. 1B). Furthermore, the uric acid levels were significantly decreased after the oral administration of BBR in both the low-dose BBR group (100 mg/kg, by 29% after 1 week of treatment and by 47% after 2 weeks of treatment, $**P < 0.01$) and the high-dose BBR group (200 mg/kg, by 48% after 1 week of treatment and by 54% after 2 weeks of treatment, $***P < 0.001$) in a time- and dose-dependent manner (Fig. 1B).

Moreover, the hypouricemic effect of BBR was confirmed in an acute xanthine-induced hyperuricemia mouse model (Fig. 1C). The level of uric acid was significantly elevated after 14 days of modeling ($**P < 0.01$, Fig. 1D) and decreased after the oral administration of BBR ($*P < 0.05$, Fig. 1D). Notably, the therapeutic effect of BBR in terms of lowering uric acid levels is similar to that of benzbromarone (a positive control drug). Furthermore, the kidneys of mice in the xanthine-induced hyperuricemia model group exhibited slight swelling, and the kidney/weight ratio in the model group was significantly greater than that in the control group ($*P < 0.05$, Fig. 1E). BBR decreased the kidney/weight ratio, which suggested that BBR protected the kidney (Fig. 1E). In addition, BBR reversed the elevation in creatinine levels in xanthine-induced hyperuricemia model mice in a dose-dependent manner ($**P < 0.01$, Fig. 1F).

Then, the uric acid-lowering effect of BBR was validated by determining the uric acid levels after single or multiple oral administrations of BBR in normal SD rats (Fig. 1G and H). As shown in Fig. 1G, after oral administration of one dose of BBR (200 mg/kg) for 6, 12 or 24 h, the plasma uric acid concentration decreased by 20%, 22% or 17%, respectively (Fig. 1H), compared with that in the control rats (no change); this result indicated that BBR may rapidly lower uric acid levels. After continuous oral administration of BBR

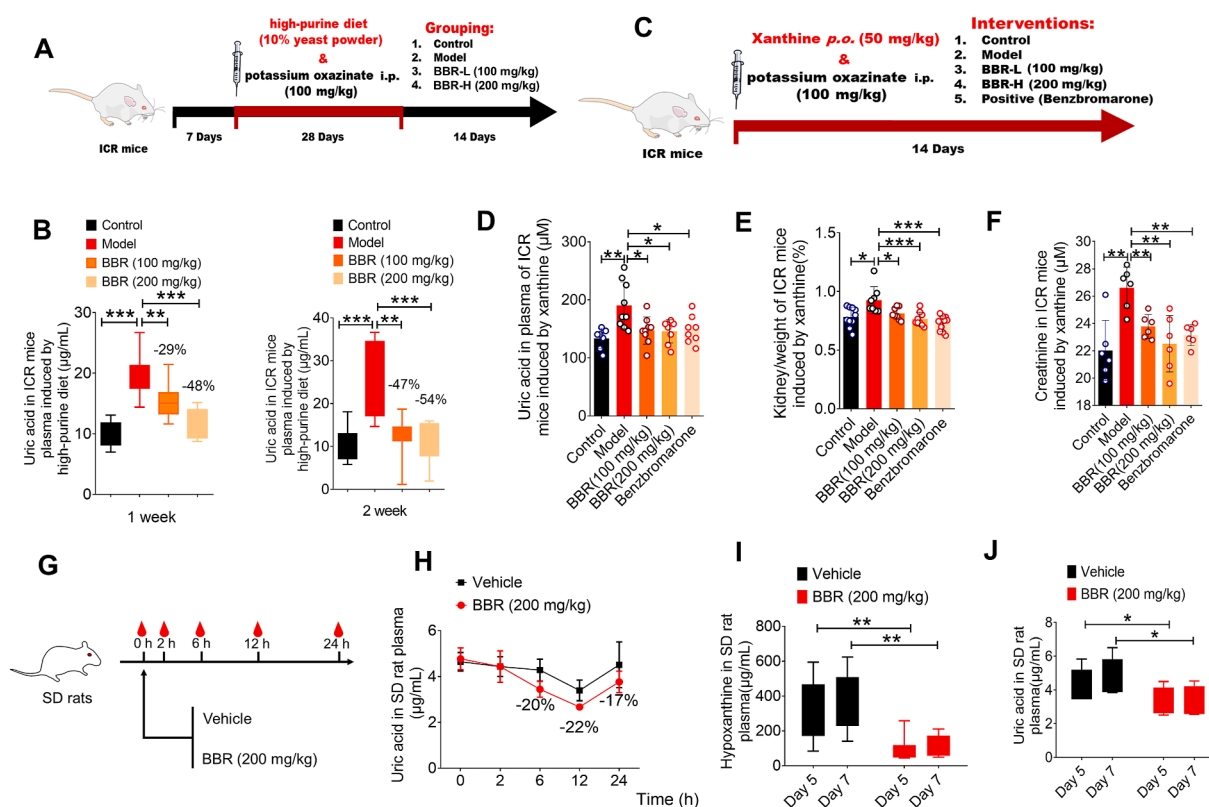


Figure 1 BBR significantly improves chronic/acute hyperuricemia in ICR mice. (A) Experimental grouping and scheme of the chronic hyperuricemia model induced by a high-purine diet. (B) Uric acid levels in the plasma after 1 week (left) and 2 weeks (right) of treatment ($n = 10$). (C) Experimental grouping and scheme of the xanthine-induced acute hyperuricemia model. (D) Uric acid level in the plasma of animals in the xanthine-induced model (Control: $n = 7$; Model: $n = 9$; BBR 100 mg/kg: $n = 9$; BBR 200 mg/kg: $n = 8$; Benzbromarone: $n = 8$). (E) Ratio of kidney weight/body weight of animals in the xanthine-induced model (Control: $n = 10$; Model: $n = 11$; BBR 100 mg/kg: $n = 9$; BBR 200 mg/kg: $n = 10$; Benzbromarone: $n = 10$). (F) Plasma creatinine level of animals in the xanthine-induced model ($n = 6$). (G, H) Experimental grouping and scheme of the single-dose oral administration of BBR group (G) and the uric acid level in the plasma ($n = 5$) (H). (I) Hypoxanthine levels in the plasma after multiple doses of oral BBR ($n = 6$). (J) Uric acid levels in the plasma after multiple doses of oral BBR ($n = 6$). The t -test is used for pairwise comparison within the group (two-sided, unpaired), the data are shown as the mean \pm SD, $*P < 0.05$, $**P < 0.01$, $***P < 0.001$.

for 5 and 7 days, hypoxanthine (the precursor of uric acid) levels in the plasma were reduced significantly (** $P < 0.01$, Fig. 1I). Moreover, the uric acid level in the BBR group also decreased (* $P < 0.05$, Fig. 1J). Due to the decrease in the level of hypoxanthine, we can infer that BBR-induced decreases in uric acid levels may be associated with the uric acid synthesis pathway.

Based on the demand for mass spectrometry detection of a large number of nucleic acid analogues in this study, we constructed a targeted LC–MS/MS detection method, and the extracted ion chromatogram of the targeted method, as well as the standard curves was shown in Supporting Information Fig. S1. The indexes of the methodological validation met the requirements, including specificity, linearity and lower limit of quantification, accuracy and precision, recovery and matrix effect and dilution linearity, and the results are displayed in Supporting Information Tables S1–S5.

3.2. BBR lowered blood uric acid levels by targeting the gut microbiota

Due to the difficulty in absorbing BBR after oral administration, BBR inevitably interacts with gut bacteria after entering the intestine. Thus, the regulatory effect of BBR on the composition of the gut microbiota in a model of chronic hyperuricemia (induced by a high-purine diet) was studied. As shown in Fig. 2A, the results of principal component analysis (PCA) showed that the structure of the intestinal flora in the hyperuricemia model group was different from that in the control group, and BBR significantly

altered the structure of the intestinal flora in the hyperuricemia state (Fig. 2A), suggesting that the gut microbiota participates in the uric acid-lowering effect of BBR. Furthermore, BBR also affected the α -diversity of the intestinal flora in the hyperuricemia model. The Chao1 index of the BBR group was significantly lower than that of the model group (Supporting Information Fig. S2A), and the Shannon index tended to decrease after BBR administration (Fig. S2B). Fig. 2B shows the composition of the intestinal flora at the phylum level. Significant differences were observed in various intestinal phyla. There was a significant decrease in the abundance of Verrucomicrobia (Fig. 2C) and a significant increase in the abundance of Actinobacteria (Fig. 2D) in the model group. Verrucomicrobia contains numerous probiotics, with *Akkermansia muciniphila* being the most well-known. BBR administration significantly increased the abundance of Verrucomicrobia and reduced the abundance of Actinobacteria, which restored the composition and function of the intestinal flora. Next, we focused on changes at the genus level. As shown in Fig. 2E, the abundance of *Anaerotruncus* was significantly reduced in the model group, while BBR increased the abundance of *Anaerotruncus*. *Anaerotruncus*, which was originally isolated from bariatric surgery patients, produces succinic acid, which can be utilized for obesity treatment²⁰. We also observed that BBR significantly reduced the abundances of *Coriobacteriaceae_UCG-002*, *Ruminococcaceae_UCG-001*, *Prevotellaceae_UCG-001* and *Allobaculum* while increasing the abundance of *Bacteroides*. As shown in Fig. 2F, *Coriobacteriaceae_UCG-002* abundance increased in the hyperuricemia state, and BBR significantly inhibited its

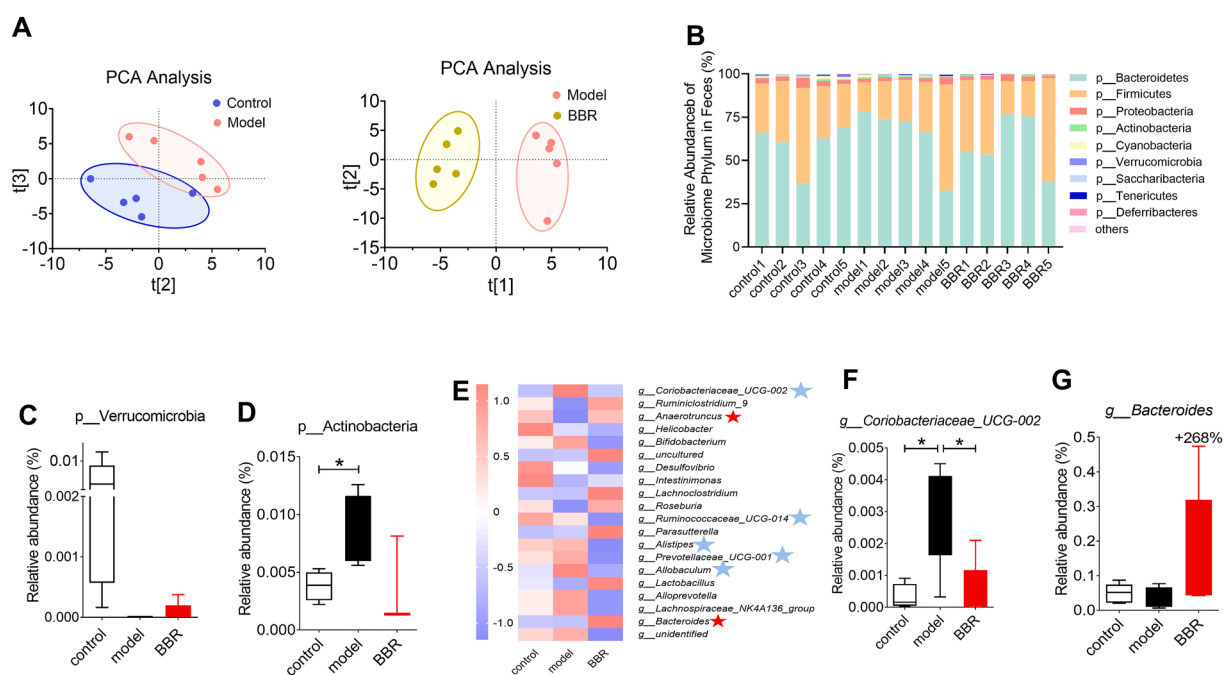


Figure 2 BBR changed the gut microbiota composition in an animal model of chronic hyperuricemia. (A) Differences in PCA analysis between the control group and the model group (left), as well as the model group and the BBR group (right). (B) Differences in the intestinal flora at the phylum level. (C) Changes in the relative abundance of the phylum Verrucomicrobia. (D) Changes in the relative abundance of the phylum Actinobacteria. (E) Heatmap of the gut microbiota at the genus level. (F) Changes in the relative abundance of the genus *Coriobacteriaceae_UCG-002*. (G) Changes in the relative abundance of the genus *Bacteroides*. The *t*-test is used for pairwise comparison within the group (two-sided, unpaired), the data are shown as the mean \pm SD, * $P < 0.05$, ** $P < 0.01$, *** $P < 0.001$, $n = 5$.

growth. Furthermore, the abundance of *Bacteroides* increased by 268% compared with that in the model group (Fig. 2G).

3.3. BBR alleviated hyperuricemia in 22 clinical subjects by increasing *Bacteroides* abundance and decreasing that of *Clostridium sensu stricto_1*

BBR has been proven to regulate glucose and lipid metabolism in the clinic^{13,15}. To determine whether BBR administration decreased serum uric acid levels in humans, 22 individuals with hyperlipidemia were randomly enrolled in a BBR treatment study in the outpatient section of the First Hospital of Jilin University in Changchun in the early spring of 2017 (clinical approval number ChiCTR-OPN-17012942). Twenty-two individuals (8 patients with hyperuricemia and 14 volunteers with normal uric acid levels; all 22 enrolled subjects had hyperlipidemia) were enrolled and given BBR as an intervention for 6 months to investigate whether BBR could decrease uric acid levels when used clinically. There were 11 males and 11 females in this trial, with an average age of 65 ± 5.9 years. The criteria for hyperuricemia were a blood uric acid concentration that exceeded $420 \mu\text{mol/L}$ for men and $360 \mu\text{mol/L}$ for women. At enrollment, the blood uric acid concentration in the hyperuricemia group was $421.6 \pm 57.52 \mu\text{mol/mL}$, and that in the non-hyperuricemia group was $320.0 \pm 65.52 \mu\text{mol/mL}$. There were significant differences between the two groups at enrollment (Supporting Information Table S6). Blood samples were collected every 2 months. During the trial, all subjects showed good tolerance to BBR, no serious adverse reactions and no drug withdrawal due to severe adverse reactions. After the administration of BBR, the average uric acid levels of all 22 subjects significantly decreased at 2 (by 6.95%, $*P < 0.05$), 4 (by 10.37%, $**P < 0.01$) and 6 months (by 11.34%, $***P < 0.001$) in a time-dependent manner (Fig. 3A, Table 1). With prolonged administration of BBR, the blood uric acid levels in patients with hyperuricemia decreased by 8.80%, 12.10% and 11.00% after taking BBR for 2, 4, and 6 months, respectively (Fig. 3B, Table 1). Furthermore, with prolonged administration of BBR, the blood uric acid levels in volunteers without hyperuricemia decreased by 5.50%, 9.10% and 12.70% after taking BBR for 2, 4, and 6 months, respectively (Fig. 3C, Table 1). In this study, with increasing BBR treatment time, the rate of decrease in uric acid levels increased. BBR has a certain ability to lower blood uric acid levels, and it is effective in both patients with hyperuricemia and subjects with normal blood uric acid levels.

At the same time, the blood creatinine and BUN levels of the enrolled subjects were also analyzed as patients with hyperuricemia are more likely to suffer renal injury with age. As shown in Fig. 3D, after taking BBR for 2, 4, or 6 months, the blood creatinine level significantly decreased in a time-dependent manner. However, BBR did not obviously reduce the blood BUN level (Fig. 3E). These results indicate that BBR also has a therapeutic effect in terms of improving renal function.

The regulatory effect of BBR on the gut microbiota in patients with hyperuricemia was also investigated. *Bacteroides* and *Clostridium sensu stricto_1* were the most variable strains identified during the experiment. At enrollment, the abundance of *Bacteroides* in patients with hyperuricemia was lower than that in volunteers without hyperuricemia (Fig. 3F), and the abundance of *Clostridium sensu stricto_1* was enriched in patients with hyperuricemia (Fig. 3G). After 6 months of treatment, the abundance of *Bacteroides* in volunteers without hyperuricemia did not change

significantly during BBR treatment (Fig. 3H). However, the abundance of *Bacteroides* in patients with hyperuricemia increased significantly in a time-dependent manner (Fig. 3I). The abundance of *Bacteroides* had a significant negative correlation with the plasma uric acid level ($R^2 = 0.3046$, $P = 0.077$) in the subjects (Fig. 3J). There was a decreasing trend in *Clostridium sensu stricto_1* abundance in both volunteers without hyperuricemia (Fig. 3K) and patients with hyperuricemia (Fig. 3L) during BBR treatment. Similarly, the abundance of *Clostridium sensu stricto_1* showed a significant positive correlation with plasma uric acid levels ($R^2 = 0.2719$, $P = 0.0128$) in subjects (Fig. 3M). Thus, BBR-induced increases in *Bacteroides* abundance and decreases in *Clostridium sensu stricto_1* abundance may be related to BBR-mediated regulation of the gut microbiota in a personalized manner, which can ameliorate hyperuricemia.

3.4. *Bacteroides fragilis* and its metabolite succinic acid elevated by BBR significantly reduced plasma uric acid levels in animal models of hyperuricemia

As the abundance of *Bacteroides* was elevated after treatment with BBR both in hyperuricemia animal models and in clinical patients, and a significant negative correlation between *Bacteroides* and blood uric acid was observed in the clinical study, we considered that *Bacteroides* may have a unique biological mechanism through which it ameliorates hyperuricemia. After obtaining basic information on the *Bacteroides* genus, we found that the *Bacteroides* genus has a remarkable ability to metabolize carbohydrates and is capable of fermenting carbohydrates to produce a variety of short-chain fatty acids (such as succinic acid and propionic acid). In this study, *Bacteroides fragilis* was selected for the experiment for the following reasons: 1) *Bacteroides fragilis* is a well-studied *Bacteroides*, and strains are relatively easy to obtain; 2) *Bacteroides fragilis* utilizes significant amounts of carbohydrates, such as fructose and polyfructose²¹⁻²³; and 3) *Bacteroides fragilis* is beneficial for the immune system in the host²⁴.

Therefore, the fructose-induced acute hyperuricemia model was chosen to evaluate the possible metabolic mechanism by which *Bacteroides* ameliorates hyperuricemia (Fig. 4A). As shown in Fig. 4B, the blood uric acid level of the model group was significantly greater than that of the control group ($**P < 0.01$), while the *Bacteroides fragilis* transplantation group ($***P < 0.001$) and the *Bacteroides fragilis* transplantation combined with BBR group ($***P < 0.001$) had significantly lower blood uric acid levels, which indicated that *Bacteroides fragilis* plays a role in regulating uric acid levels.

Then, we determined the levels of SCFAs in the feces. As shown in Fig. 4C and D, the succinic acid content in the fecal samples of model mice decreased significantly, while that in the *Bacteroides fragilis* group and the combination of *Bacteroides fragilis* and BBR group significantly increased (Fig. 4C). The content of propionic acid in the feces was also significantly increased following *Bacteroides fragilis* intervention or treatment with the combination of *Bacteroides fragilis* and BBR (Fig. 4D). The abundances of both succinic acid ($R^2 = 0.3361$, $P = 0.0074$, Fig. 4E) and propanoic acid ($R^2 = 0.2496$, $P = 0.0249$, Fig. 4F) showed a significant negative correlation with plasma uric acid levels. Interestingly, we observed that *Bacteroides fragilis* lowered blood uric acid levels in the context of hyperuricemia, which may be related to the elevated production of short-chain fatty acids, especially succinic acid.

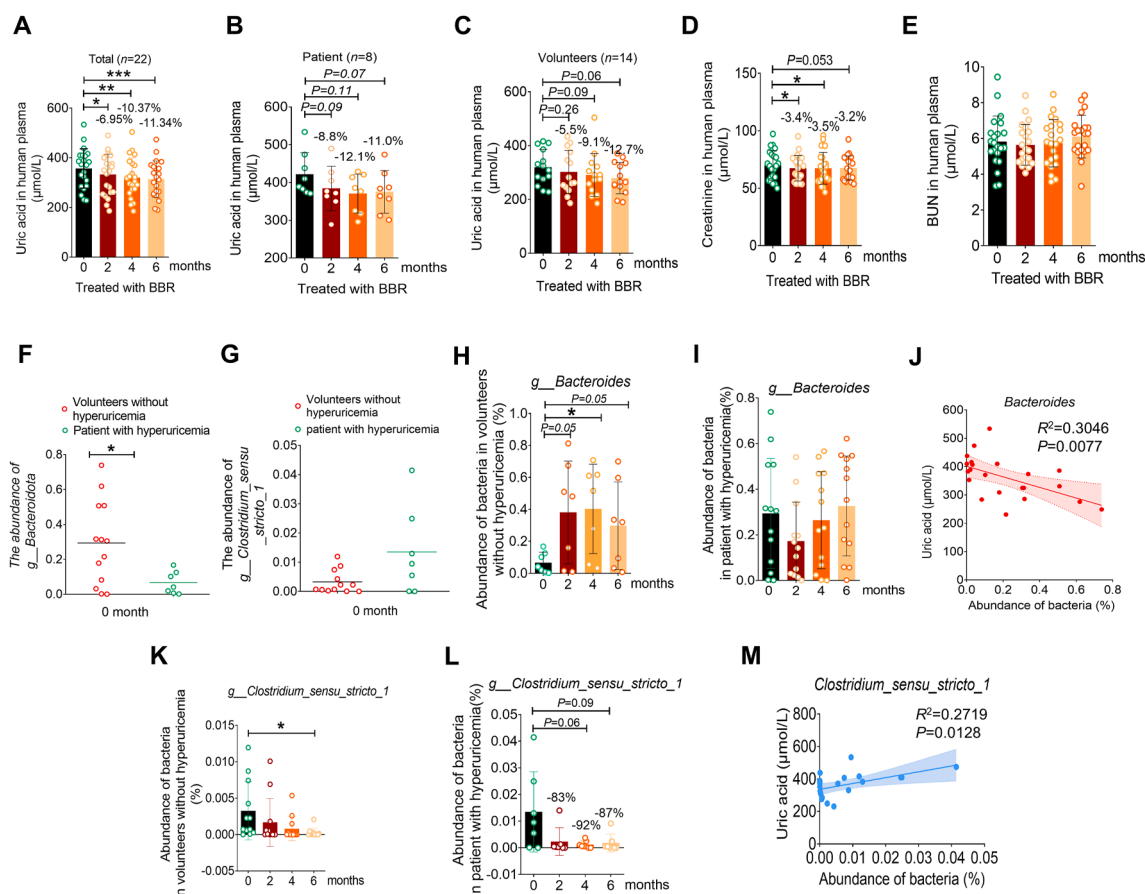


Figure 3 BBR alters the gut microbiota composition in patients with hyperuricemia. (A) Uric acid levels in 22 subjects after 2, 4 and 6 months of treatment with BBR. (B) Uric acid levels in 8 patients with hyperuricemia. (C) Uric acid levels in 14 volunteers without hyperuricemia. (D) Creatinine levels in 22 subjects after 2, 4 and 6 months of treatment with BBR. (E) BUN levels in 22 subjects after 2, 4 and 6 months of treatment with BBR. (F) Abundance of *Bacteroides* in hyperuricemia patients and volunteers without hyperuricemia at enrollment. (G) Abundance of *Clostridium_sensu_stricto_1* in hyperuricemia patients and volunteers without hyperuricemia at enrollment. (H) Abundance of *Bacteroides* in volunteers without hyperuricemia after 2, 4 and 6 months of treatment with BBR ($n = 7$). (I) Abundance of *Bacteroides* in hyperuricemia patients after 2, 4 and 6 months of treatment with BBR ($n = 13$). (J) Correlation analysis of the abundance of *Bacteroides* and the uric acid level in subjects. (K) Abundance of *Clostridium_sensu_stricto_1* in volunteers without hyperuricemia after 2, 4 and 6 months of treatment with BBR ($n = 12$). (L) Abundance of *Clostridium_sensu_stricto_1* in hyperuricemia patients after 2, 4 and 6 months of treatment with BBR ($n = 7$). (M) Correlation analysis of the abundance of *Clostridium_sensu_stricto_1* and the uric acid level in the subjects. The t -test is used for pairwise comparison within the group (two-sided, unpaired). The data are shown as the mean \pm SEM, * $P < 0.05$, ** $P < 0.01$, *** $P < 0.001$.

Thus, the therapeutic effect of succinic acid on hyperuricemia was further investigated. Sodium succinate was administered to model animals with fructose-induced (Fig. 4G) hyperuricemia. With the administration of sodium succinate, the uric acid level decreased (Fig. 4H). Furthermore, the hepatic phosphate level slightly increased following sodium succinate administration (Fig. 4I), leading to the inhibition of AMP2D activity (Fig. 4J). However, the regulatory effect of sodium succinate was weaker than that of BBR, suggesting that sodium succinate may also regulate hyperuricemia *via* other pathways. Analysis of the uric acid synthesis pathway showed that the levels of most metabolites (AMP, IMP, inosine, hypoxanthine and xanthine) in the pathway in both the fructose-induced and sodium glutamate-induced models decreased due to the administration of sodium succinate (Fig. 4K–O); thus, we can infer that succinic acid may play an important role in regulation of the uric acid synthesis pathway, which can alleviate hyperuricemia.

3.5. BBR inhibits uric acid synthesis pathway by reducing liver AMP2D activity and increasing phosphate levels in the body through intestinal succinic acid

To clarify the mechanism underlying the hypouricemic activity of BBR, we incubated BBR with xanthine oxidase, and the classic xanthine oxidase inhibitor febuxostat was used as a positive control. As shown in Supporting Information Fig. S3, the rate of inhibition of xanthine oxidase by febuxostat was 24.52% at 10^{-7} mol/L and 63.91% at 10^{-6} mol/L. However, BBR did not have an obvious inhibitory effect at 10^{-4} mol/L, with an inhibition rate of only 0.043%; this result indicated that BBR is not a direct inhibitor of xanthine oxidase.

Then, we investigated whether BBR impacted the uric acid synthesis pathway. A sodium glutamate-induced hyperuricemia model with abnormal uric acid metabolism was established (Fig. 5A). The principle underlying the sodium glutamate-induced hyperuricemia model is as follows. Excess glutamate is

Table 1 The serum uric acid of patients before and after BBR treatment.

Group	Participant No.	Code	Serum uric acid ($\mu\text{mol/L}$)				
			Before treatment ^a		After treatment ^b		
					2 months	4 months	6 months
Hyperuricemia group ($n = 8$)	1	L JM	374	372	318	312	
	2	L QC	534	427	429	387	
	3	F XL	389	377	414	384	
	4	L R	383	364	377	357	
	5	C JR	438	405	386	424	
	6	C LJ	474	490	421	474	
	7	C GQ	410	350	325	301	
	8	Y XY	371	289	296	364	
Mean \pm SD ($n = 8$)			421.6 \pm 57.52	384.3 \pm 58.92	370.8 \pm 51.44	375.4 \pm 56.46	
% of reduction ^a : $(b-a)/a \times 100$			—	8.80%	12.10%	11.00%	
Non hyperuricemia group ($n = 14$)	9	Y GY	410	376	370	335	
	10	Y ZY	249	186	185	190	
	11	L ZF	416	410	336	339	
	12	C K	325	282	273	252	
	13	T WM	342	245	305	248	
	14	W YH	331	336	291	288	
	15	K LH	386	434	504	371	
	16	Z LY	276	260	258	264	
	17	L CX	286	262	275	226	
	18	W SC	231	253	235	255	
	19	S HB	284	346	292	323	
	20	Y CR	407	400	322	357	
	21	S LT	228	209	216	195	
	22	Q SF	309	234	211	266	
Mean \pm SD ($n = 14$)			320.0 \pm 65.52	302.4 \pm 80.10	290.9 \pm 79.84	279.2 \pm 58.01	
% of reduction ^a : $(b-a)/a \times 100$			—	5.50%	9.10%	12.70%	
Mean \pm SD ($n = 22$)			357.0 \pm 79.15	332.1 \pm 82.19	320.0 \pm 79.83	314.2 \pm 73.40	
% of reduction ^a : $(b-a)/a \times 100$			—	6.95%	10.37%	11.34%	

^aAbsolute value.

metabolized into glutamine in the liver and hypothalamus and ultimately into IMP through the purine pathway while consuming ATP and generating AMP; AMP then enters the purine degradation pathway to generate uric acid *via* AMPD2²⁵. The uric acid content in the model group was significantly greater than that in the control group ($***P < 0.001$, Fig. 5B), and BBR significantly lowered the blood uric acid level in a dose-dependent manner ($***P < 0.001$). Additionally, metabolites in the uric acid synthesis pathway (Fig. 5C) were analyzed by LC-MS/MS. As shown in Fig. 5D–H, the plasma AMP level in the model group was significantly decreased ($**P < 0.01$, Fig. 5D), and both the high doses of BBR and succinic acid significantly restored the level of AMP ($***P < 0.001$, Fig. 5D). Furthermore, the IMP level in the model group was significantly greater than that in the control group ($**P < 0.01$, Fig. 5E). BBR reversed the increase in IMP (Fig. 5E). Finally, as shown in Fig. 5F–H, the levels of the downstream metabolites of IMP, including inosine ($***P < 0.001$, Fig. 5F), hypoxanthine ($**P < 0.01$, Fig. 5G), and xanthine (Fig. 5H), were increased in the model group, from which we can infer that the IMP pathway was enriched in the hyperuricemia state. Similarly, BBR significantly decreased the levels of inosine (Fig. 5F), hypoxanthine (Fig. 5G) and xanthine (Fig. 5H), which proved that BBR regulated the uric acid pathway, especially the flux of AMP to IMP.

As the AMPD2 protein is responsible for the conversion of AMP to IMP in this pathway, evaluating the influence of BBR on AMPD2 is necessary. The process for evaluating AMPD2 activity

was based on previous reports with some modifications²⁶. Briefly, AMP was added to a freshly prepared liver homogenate and the sample was incubated for 15 min. As IMP is rapidly metabolized to inosine in the system and it is difficult to track the changes in intermediates, the decomposition rate of AMP and the generation rate of inosine were considered to represent AMPD2 activity. In this study, liver AMPD2 activity in sodium glutamate-induced hyperuricemia model mice was reduced after BBR treatment (Fig. 5I). Also as shown in Fig. 5D–F, the rate of AMP reduction in the model group was significantly greater than in the control group ($**P < 0.01$, Fig. 5D); furthermore, BBR remarkably slowed this transformation process ($***P < 0.001$, Fig. 5D). Similarly, the rate of inosine generation in the model group significantly increased ($***P < 0.001$, Fig. 5F), and BBR treatment clearly reduced this rate ($*P < 0.05$, Fig. 5F). Hepatic phosphate is a natural inhibitor of AMPD2^{27,28}. Here, we measured the hepatic phosphate level (Fig. 5J). The hepatic phosphate concentration in the model group decreased significantly compared to that in the control group ($*P < 0.05$, Fig. 5J), but BBR obviously reversed this effect and significantly elevated the phosphate concentration ($*P < 0.05$, Fig. 5J). Thus, BBR may endogenously inhibit the activity of hepatic AMPD2 by increasing the phosphate concentration in hepatocytes.

Although the above results suggested that BBR could reduce uric acid synthesis by inhibiting liver AMPD2, an important question appeared that BBR was difficult to absorb and had low exposure in the liver²⁹. Since *Bacteroides fragilis* and its

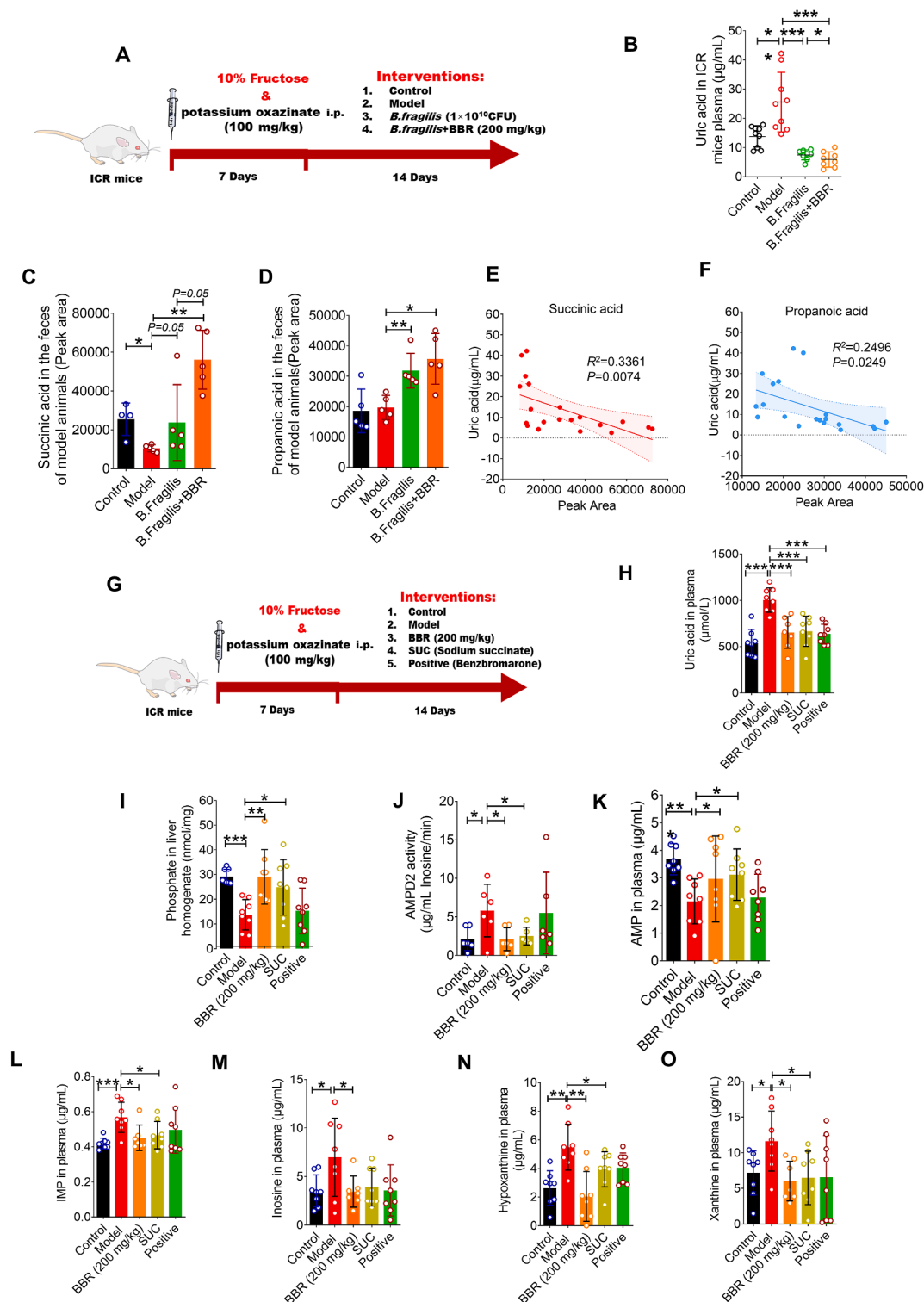


Figure 4 *Bacteroides fragilis* and its metabolite succinic acid significantly reduced plasma uric acid levels in animal models of hyperuricemia. (A) Experimental grouping and scheme of the study of *Bacteroides fragilis* in the fructose-induced hyperuricemia model. (B) Uric acid levels in the *Bacteroides fragilis*-treated hyperuricemia model animals (Control: $n = 9$; Model: $n = 9$; *B. fragilis*: $n = 8$; *B. fragilis* + BBR: $n = 8$). (C) The succinic acid content in the feces of the *Bacteroides fragilis*-treated hyperuricemia model animals ($n = 5$). (D) The propanoic acid content in the feces of the *Bacteroides fragilis*-treated hyperuricemia model animals ($n = 5$). (E) Correlation analysis of the contents of succinic acid and uric acid. (F) Correlation analysis of the content of propanoic acid and the uric acid level. (G) Experimental grouping and scheme for the study of sodium succinate in the fructose-induced hyperuricemia model. (H) Uric acid levels after sodium succinate administration in the fructose-induced hyperuricemia model (Control: $n = 8$; Model: $n = 8$; BBR 200 mg/kg: $n = 7$; SUC: $n = 8$; Positive: $n = 8$). (I) Hepatic phosphate levels after fructose-induced sodium succinate administration in the hyperuricemia model ($n = 8$). (J) AMPD2 activity evaluated based on the rate of inosine

metabolite succinic acid elevated by BBR significantly reduced plasma uric acid levels in animal models of hyperuricemia, we hypothesized that succinic acid may inhibit liver AMPD2 activity, leading to a decrease level in uric acid in BBR. Based on the hypothesis above, the effect of succinic acid on the uric acid synthesis pathway at the cellular level was further investigated to validate the direct lowering-uric acid effect and mechanism of succinic acid. The cytotoxicity of succinic acid was evaluated using the HEK 293T cell lines to determine the appropriate concentration for further study (Supporting Information Fig. S4). As a result, succinic acid was used at concentrations no greater than 2.5 mmol/L in HEK 293T cells. Then, to validate succinic acid regulation of the uric acid synthesis pathway, HEK 293T cells were incubated with a serial concentration of succinic acid (0.625, 1.25 and 2.5 mmol/L) for 24 h respectively, as 293T cells were well tolerant to succinic acid. As shown in Fig. 5K–R, uric acid was significantly decreased ($***P < 0.001$, Fig. 5K) under high dosage of succinic acid, while the phosphate level was inhibited ($***P < 0.001$, Fig. 5L). Other metabolites in the uric acid synthesis pathway also showed corresponding changes, the ATP content significantly decreased ($***P < 0.001$, Fig. 5M), and the AMP content significantly increased ($***P < 0.001$, Fig. 5N). Moreover, the levels of IMP ($***P < 0.001$, Fig. 5O), inosine ($***P < 0.001$, Fig. 5P), hypoxanthine ($***P < 0.001$, Fig. 5Q), and xanthine ($***P < 0.001$, Fig. 5R) were significantly decreased, suggesting that the therapeutic effect of succinic acid was related to regulation of the uric acid synthesis pathway. Furthermore, fructose was added to the medium to quickly deplete intracellular phosphate, and succinic acid at two dosages of 0.625 or 2.5 mmol/L respectively significantly restored the phosphate level in a dose-dependent manner (Fig. 5S). Similarly, the fructose-induced increase in ATP was reversed by succinic acid (Fig. 5T).

Overall, we can infer that disturbance of the intracellular ATP content by succinic acid can significantly alter the intracellular phosphate pool, thereby increasing the concentration of intracellular free phosphate, which is an endogenous inhibitor of AMPD2. The uric acid synthesis pathway was inhibited, and uric acid levels are decreased (Fig. 5U).

3.6. BBR can prevent renal damage caused by hyperuricemia

The results of the above study showed that BBR administration decreased the creatinine level in xanthine-induced acute hyperuricemia model animals and in clinical patients, suggesting that BBR has renal protective effects. As hyperuricemia often disrupts renal function, the effect of BBR on nephropathy in patients with hyperuricemia should be investigated.

First, a nephropathy rat model of hyperuricemia was established by feeding rats 10% yeast powder and 0.15% adenine for more than six weeks (Fig. 6A). After successful modeling, the uric acid level in the blood of the model group was significantly greater than that in the blood of the control group ($**P < 0.01$, Fig. 6B). Febuxostat (10 mg/kg) was used as a positive control drug and significantly reduced blood uric acid levels ($***P < 0.001$, Fig. 6B). Both low-dose (100 mg/kg) and high-dose (200 mg/kg) BBR significantly

reduced blood uric acid levels in a dose-dependent manner (Fig. 6B). HE staining demonstrated that compared to those in the control group, there was obvious damage to nephrons with many vacuoles and the deposition of urate crystals in the model group (Fig. 6C). Low-dose and high-dose BBR, as well as febuxostat, significantly alleviated the renal damage caused by high levels of uric acid with reduced vacuoles and urate crystals, showing obvious renal protection effects (Fig. 6C). The blood creatinine ($***P < 0.001$, Fig. 6D) and BUN ($**P < 0.01$, Fig. 6E) levels in the model group were also significantly greater than those in the control group. Both low-dose and high-dose BBR, as well as febuxostat, significantly reduced the blood creatinine (Fig. 6D) and BUN (Fig. 6E) levels; this result was consistent with the renoprotective effect of BBR in the clinical study.

Next, we quantified level of xanthine in plasma. As shown in Fig. 6F, the level of xanthine in the model group was significantly greater than that in the control group ($***P < 0.001$), indicating the accumulation of xanthine in model rats with nephropathy and hyperuricemia. Febuxostat is a strong xanthine oxidase inhibitor that inhibits the conversion of xanthine into uric acid; as such, an increased level of xanthine in the febuxostat group ($***P < 0.001$) was observed. Moreover, the xanthine level showed a decreasing trend in both the high- ($**P < 0.01$) and low-dose ($*P < 0.05$) BBR groups, while BBR decreased uric acid levels; this result was consistent with the fact that BBR is not a xanthine oxidase inhibitor (Fig. S3) and acts by regulating the uric acid synthesis pathway.

TMAO is an intestinal-derived metabolite of the intestinal flora that is closely related to cardiovascular disease and kidney disease³⁰. As shown in Fig. 6G, TMAO accumulated in the model group ($***P < 0.001$). Low-dose ($**P < 0.01$) and high-dose ($*P < 0.05$) BBR, as well as febuxostat ($***P < 0.001$), significantly reduced the concentration of TMAO in the blood, which confirmed the renoprotective effect of BBR.

4. Discussion

Hyperuricemia is a metabolic disease caused by disordered purine nucleic acid metabolism and the abnormal excretion of uric acid. The comprehensive incidence rate of hyperuricemia (5.5%–23.6%), the trend toward a younger age of onset and the large number of complications accompanying hyperuricemia have greatly affected people's quality of life². Current clinical first-line drugs indicated for hyperuricemia treatment include allopurinol, febuxostat and benzbromarone. However, side effects (hypersensitivity from allopurinol and increased cardiovascular risk from febuxostat, which is sometimes lethal), contraindications (benzbromarone), and economic burdens (febuxostat) affect the clinical use of existing drugs^{7,31}. Therefore, finding safe and effective candidate compounds for the treatment of hyperuricemia is important. The intestinal tract is closely related to the metabolism of uric acid³². The uric acid transporter in the intestinal tract mediates the excretion of 1/3 of all uric acid⁵. At the same time, the gut microbiota in the intestinal tract plays a role in uric acid homeostasis in the host by participating in nucleic acid metabolism and the decomposition of uric acid^{33,34}. Thus, the intestinal

generation ($n = 6$). (K–O) The plasma levels of AMP ($n = 8$) (K), IMP (Control: $n = 8$; Model: $n = 8$; BBR 200 mg/kg: $n = 7$; SUC: $n = 8$; Positive: $n = 8$) (L), inosine (Control: $n = 8$; Model: $n = 8$; BBR 200 mg/kg: $n = 7$; SUC: $n = 8$; Positive: $n = 8$) (M), hypoxanthine ($n = 8$) (N), and xanthine (Control: $n = 8$; Model: $n = 8$; BBR 200 mg/kg: $n = 7$; SUC: $n = 8$; Positive: $n = 8$) (O). The *t*-test is used for pairwise comparison within the group (two-sided, unpaired). The data are shown as the mean \pm SD, $*P < 0.05$, $**P < 0.01$, $***P < 0.001$.

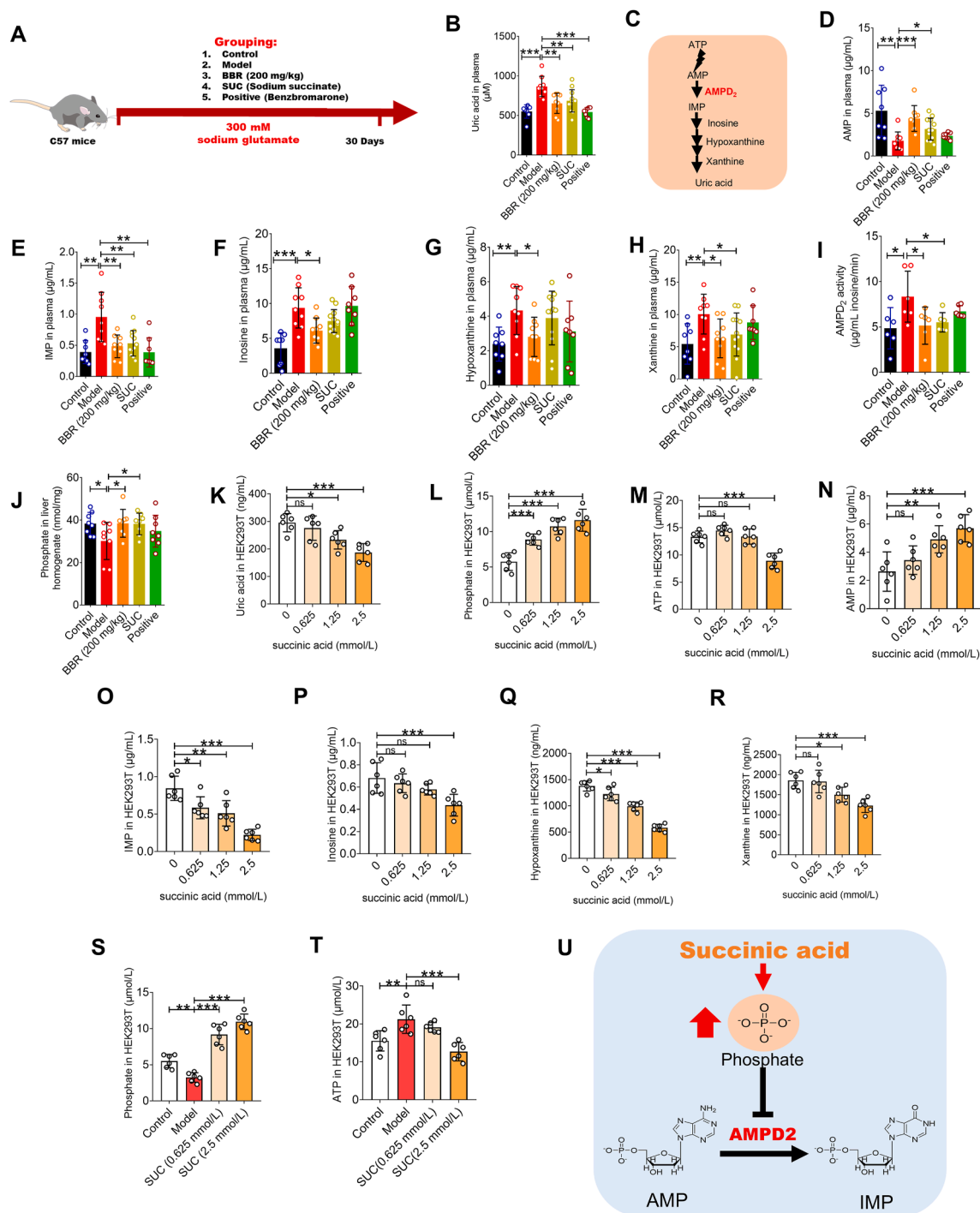


Figure 5 BBR inhibits uric acid synthesis pathway by reducing liver AMPD2 activity and increasing phosphate levels *in vivo* through the intestinal succinic acid. (A) Experimental grouping and scheme of the model of hyperuricemia induced by sodium glutamate. (B) Uric acid level in the plasma (Control: $n = 8$; Model: $n = 9$; BBR 200 mg/kg: $n = 9$; SUC: $n = 12$; Positive: $n = 8$). (C) Illustration of the uric acid synthesis pathway. (D) AMP level in the plasma (Control: $n = 8$; Model: $n = 9$; BBR 200 mg/kg: $n = 9$; SUC: $n = 12$; Positive: $n = 8$). (E) IMP level in the plasma (Control: $n = 8$; Model: $n = 9$; BBR 200 mg/kg: $n = 9$; SUC: $n = 12$; Positive: $n = 8$). (F) Inosine level in the plasma (Control: $n = 8$; Model: $n = 9$; BBR 200 mg/kg: $n = 9$; SUC: $n = 12$; Positive: $n = 8$). (G) Hypoxanthine level in the plasma (Control: $n = 8$; Model: $n = 9$; BBR 200 mg/kg: $n = 9$; SUC: $n = 12$; Positive: $n = 8$). (H) Xanthine level in the plasma (Control: $n = 8$; Model: $n = 9$; BBR 200 mg/kg: $n = 9$; SUC: $n = 12$; Positive: $n = 8$). (I) AMPD2 activity in liver homogenate (Control: $n = 8$; Model: $n = 9$; BBR 200 mg/kg: $n = 9$; SUC: $n = 12$; Positive: $n = 8$). (J) Hepatic level of phosphate (Control: $n = 8$; Model: $n = 9$; BBR 200 mg/kg: $n = 9$; SUC: $n = 12$; Positive: $n = 8$). (K) Uric acid level in 293T cells ($n = 6$). (L) Intracellular phosphate levels in 293T cells ($n = 6$). (M) ATP levels in 293T cells ($n = 6$). (N) AMP levels in 293T cells ($n = 6$). (O) IMP levels in 293T cells ($n = 6$). (P) Inosine levels in 293T cells ($n = 6$). (Q) Hypoxanthine levels in 293T cells ($n = 6$). (R) Xanthine levels in 293T cells ($n = 6$). (S) Intracellular phosphate levels in 293T cells with succinic acid of 0.625

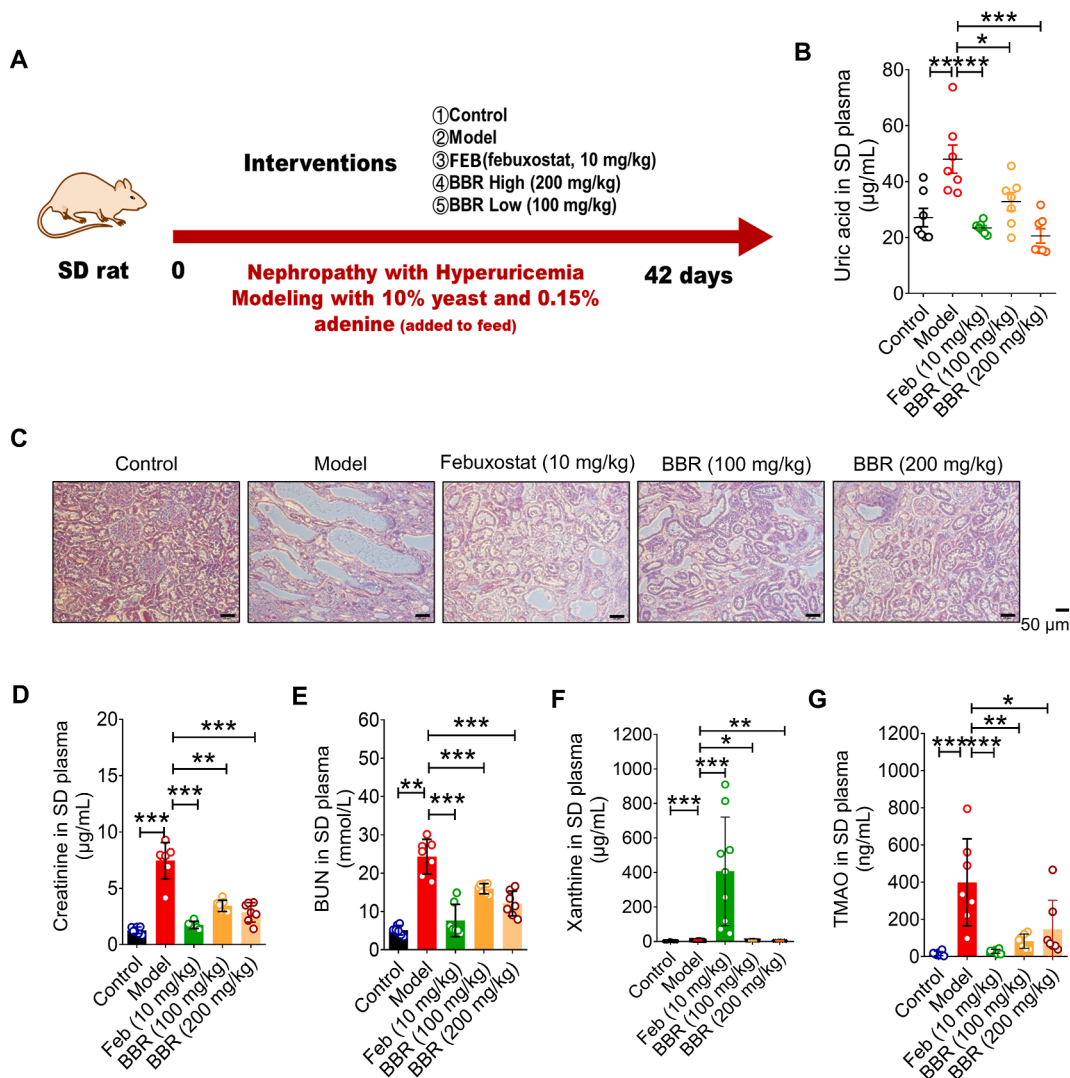


Figure 6 BBR exhibited a renal protective effect in models of nephropathy with hyperuricemia. (A) Experimental grouping and scheme of the nephropathy with hyperuricemia model. (B) Uric acid levels in the plasma ($n = 7$). (C) HE staining results of the kidneys (scale bar, 50 μm). (D) Creatinine levels in the plasma ($n = 7$). (E) BUN levels in the plasma ($n = 7$). (F) Xanthine levels in the plasma (Control: $n = 10$; Model: $n = 9$; Feb 10 mg/kg: $n = 10$; BBR 100 mg/kg: $n = 10$; BBR 200 mg/kg: $n = 9$). (G) TMAO levels in the plasma ($n = 7$). The *t*-test is used for pairwise comparison within the group (two-sided, unpaired). The data are shown as the mean \pm SD, * $P < 0.05$, ** $P < 0.01$, *** $P < 0.001$.

tract and the gut microbiota may be targets for regulating uric acid levels.

The therapeutic effect of BBR on lipid metabolism¹⁹ and glucose metabolism³⁵ suggests its potential application in the treatment of metabolic diseases³⁶. The low bioavailability and powerful bacterial-regulatory effect of BBR lead to the unique therapeutic mechanism of action of BBR in metabolic syndromes^{14,16}. BBR was first reported to have its metabolism regulated by the gut microbiota, which converts BBR into more absorbable forms³⁷. Notably, interindividual differences in gut microbiota composition result in substantial variations in the bioavailability of BBR, thereby influencing its efficacy in the personalized treatment of hyperlipidemia³⁸. In recent years,

increasing evidence has demonstrated that BBR exerts its therapeutic effects by modulating microbiota-derived endogenous metabolites. For instance, BBR ameliorates atherosclerosis by inhibiting the TMA–TMAO pathway and alleviates chronic kidney disease by suppressing intestinal *p*-cresol production^{14,16}. Due to its unique microbiota-mediated mechanisms, BBR exhibits a multi-target and multi-efficacy pharmacological profile, highlighting its potential for the treatment of various metabolic disorders.

In this study, BBR significantly regulated nucleic acid metabolism. The therapeutic effect of BBR on hyperuricemia was confirmed in both preclinical and clinical studies. Although the ability of BBR to lower blood uric acid seems relatively mild in clinical studies, its therapeutic effect against hyperuricemia is long-

or 2.5 mmol/L ($n = 6$). (T) ATP levels in 293T cells with succinic acid of 0.625 or 2.5 mmol/L ($n = 6$). (U) Illustration of succinic acid inhibition of AMPD2 mediated by increasing the intracellular phosphate level. *t*-test is used for pairwise comparison within the group (two-sided, unpaired). The data are shown as the mean \pm SD, ** $P < 0.01$, *** $P < 0.001$.

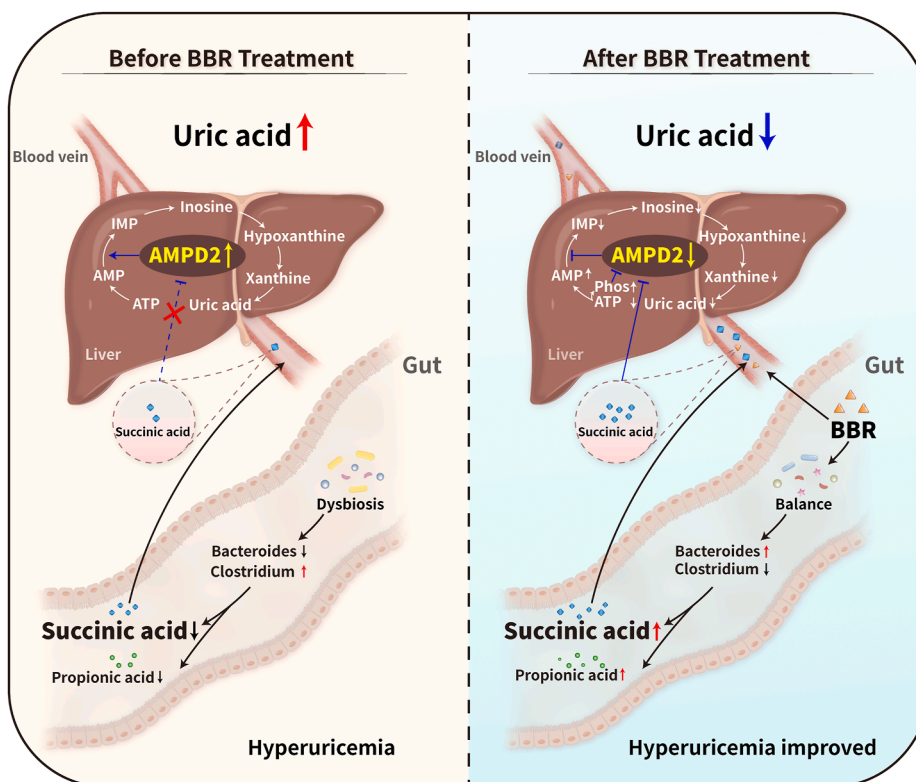


Figure 7 BBR is a promising drug for the treatment of hyperuricemia based on the inhibition of hepatic AMPD2, which is triggered by the gut microbiota.

lasting. Considering the complications accompanying hyperuricemia, the multitarget and broad-spectrum effects of BBR on regulating glucose and lipid metabolism provide BBR advantages in restoring homeostasis and alleviating hyperuricemia with a good safety profile. Moreover, BBR demonstrated excellent protective effects against renal dysfunction in animal models of nephropathy with hyperuricemia, which indicated that BBR is a good candidate for alleviating hyperuricemia and kidney dysfunction.

Here, we identified a unique mechanism by which BBR lowers uric acid levels through the gut–liver axis, which is different from that of traditional xanthine oxidase inhibitors. BBR can restructure the composition of the intestinal flora and increase the abundance of *Bacteroides* strains, which increases the production of succinic acid and thus reduces the production of uric acid in the liver. Furthermore, BBR can inhibit the activity and expression of the AMPD2 protein *via* its metabolite succinic acid, which is responsible for converting AMP to IMP in the liver, leading to a decrease in uric acid levels.

Adenosine monophosphate deaminase is the key protein in the uric acid synthesis pathway³⁹. A study on fructose and uric acid showed that high fructose consumption significantly increased the activity of AMPD2, causing a large amount of AMP to enter the degradation pathway to produce uric acid⁴⁰. A genetic polymorphism study revealed that genetic variation in glucokinase regulator protein (GCKR) leads to a decrease in the inhibitory effect of glucokinase, which in turn promotes glucose phosphorylation, resulting in ATP depletion and increased uric acid production through the AMPD2 pathway⁴¹. The flux of the uric acid pathway significantly increased in our hyperuricemia models, especially the flux of AMP conversion to IMP. AMPD2 activity significantly increased in the hyperuricemia model, and BBR effectively

inhibited AMPD2 activity and expression, suggesting that AMPD2 could play a role in BBR-mediated regulation of hyperuricemia. AMPD2 was shown to effectively control the ATP/AMP content ratio^{42,43}. Here, we found that BBR decreased the ATP level and increased the AMP level. An increase in the intrahepatic phosphate concentration was found in response to BBR, which further inhibited the activity of AMPD2 as phosphate is the most direct endogenous inhibitor of AMPD2 activity. AMPD2 antagonizes the adenosine 5'-monophosphate-activated protein kinase (AMPK) protein and regulates energy metabolism⁴³, which is mediated by uric acid. Recent studies have shown that the activation or overexpression of AMPD2 is associated with increased hepatic gluconeogenesis by decreasing AMPK activation and upregulating the expression of the rate-limiting enzymes phosphoenolpyruvate carboxykinase and glucose-6-phosphatase⁴⁴. AMPK agonists may also act as AMPD2 inhibitors to regulate uric acid levels^{26,28}. Energy storage in hibernating animals depends on the interaction between AMPD2 and AMPK in the liver²⁶. In summer, overexpression of AMPD2 leads to the production of large amounts of uric acid, which inhibits AMPK and results in the storage of large amounts of fat in the liver. In winter, the opposite situation occurs. BBR has been reported to be an activator of AMPK, which may also explain the inhibitory effect of BBR on AMPD2⁴⁵. At present, there is no clinical drug that specifically targets AMPD2 to lower uric acid levels. Based on the results of this study, we propose the use of BBR as a therapeutic candidate that may act on the target of AMPD2 to regulate uric acid levels; BBR is the first candidate with this mechanism of action.

Previous reports indicate that the gut microbiota participates in the regulation of uric acid in the host¹⁰. The intestinal flora can use uric acid as an optional carbon source or a single carbon source to

survive¹⁰. Some symbiotic bacteria, such as *Lactobacillus* and *Pseudomonas*, express uricase, allantoinase and allantoinase, which participate in the decomposition of uric acid⁴⁶. Under the action of the gut flora, uric acid is eventually metabolized into oxalate, urea and glycine. In this study, for the first time, *Bacteroides* and *Clostridium sensu stricto_1* were found to be significantly correlated with the plasma uric acid level.

Clostridium sensu stricto_1 was significantly enriched in hyperuricemia patients and its abundance was greatly reduced after BBR treatment, suggesting that *Clostridium sensu stricto_1* may contribute to the pathogenesis of hyperuricemia. *Clostridium sensu stricto_1* belongs to the Firmicutes phylum and is a gram-positive bacterium. *Clostridium acidurici*, *Clostridium cylindrosporium* and *Clostridium purinilyticum* are representatives of *Clostridium* that can decompose purine and use purine as the sole carbon, nitrogen and energy source. Thus, we infer that in the disease state of hyperuricemia, the intestinal tract is more likely to be enriched in gut flora that utilize uric acid, which provides an advantageous ecological niche for *Clostridium*^{47,48}. Furthermore, gram-positive *Clostridium* spp. is more sensitive to BBR, which may explain the decrease in *Clostridium* spp. after BBR treatment. Our previous study also demonstrated that *Clostridium* spp., which contain a series of enzymes that convert tyrosine into renal toxins, including *p*-cresol, are enriched in the gut of chronic kidney disease model animals, leading to kidney damage. BBR can reduce the abundance of *Clostridium* and inhibit the tyrosine→*p*-cresol→*p*-cresol sulfate pathway to ameliorate chronic kidney disease¹⁶; this finding is consistent with the renoprotective effect of BBR in animal models of nephropathy with hyperuricemia.

Bacteroides is a common genus of intestinal bacteria that can decompose complex polysaccharides in the diet or the intestinal mucosal layer⁴⁹. Moreover, *Bacteroides* can consume excess oxygen in the intestine, which is beneficial for the growth of anaerobic bacteria in the intestine⁵⁰. Moreover, *Bacteroides* contains gene clusters that degrade polysaccharide compounds to produce energy. In this study, the abundance of *Bacteroides* was significantly negatively correlated with the plasma uric acid level. At the same time, with the continuous administration of BBR, the abundance of *Bacteroides* increased significantly, and the blood uric acid level in clinical patients was significantly reduced. Fecal transplantation of *Bacteroides fragilis* into hyperuricemic model mice resulted in a significant reduction in uric acid levels. In this study, succinic acid and propionic acid levels were elevated after oral administration of *Bacteroides fragilis*. Both propionic acid and succinic acid can be metabolized by Bacteroidetes, but due to the widespread use of propionic acid as a substrate for gluconeogenesis in the liver/intestine, its concentration in peripheral areas such as blood is very low. Moreover, succinic acid is mainly produced by Bacteroidetes, and its intestinal and plasma concentrations are relatively easy to reach the activation concentration of its receptors. So, we focused solely on succinic acid. Oral administration of sodium succinate can also significantly reduce the blood uric acid levels in various hyperuricemia model mice. Previous reports have shown that succinic acid may be beneficial for treating hyperuricemia³⁶. *Bacteroides fragilis* has been reported to regulate host immune function by releasing outer membrane vesicles, delivering the immunomodulatory polysaccharide A to immune cells, and inducing the production of IL-10⁵¹. A recent study also revealed that oral administration of *Bacteroides fragilis* attenuated renal fibrosis by decreasing the lipopolysaccharide content, increasing the level of 1,5-anhydroglucitol, and inhibiting oxidative stress and

inflammation⁵². Other studies on other diseases also show that *Bacteroides fragilis* reduces the level of uric acid in models of autism spectrum disorder⁵³, indicating that *Bacteroides fragilis* regulates nucleic acid metabolism pathways in the body. Furthermore, *Bacteroides* can metabolize saccharides into short-chain fatty acids, which can tightly regulate glucose and lipid metabolism and reduce inflammation⁵⁴. Succinic acid was reported to promote the specification of tuft cells to suppress ileal inflammation⁵⁵. In this study, the liver of high uric acid model mice after oral administration of sodium succinate was studied, and it was found for the first time that AMPD2 was significantly inhibited by sodium succinate, resulting in a reduction in downstream uric acid production, which may be one of the pathways for succinate to intervene in the metabolism of uric acid "gut–liver" axis.

5. Conclusions

BBR demonstrated significant uric acid-lowering effects in both animal models and clinical cohorts. It increased succinate levels by upregulating the abundance of *Bacteroidetes*, and succinate inhibits AMPD2 activity in the liver to reduce uric acid levels (Fig. 7). BBR also demonstrated excellent renoprotective effects, improving nephropathy associated with hyperuricemia. Based on the evidence above, BBR could be a promising drug for the treatment of hyperuricemia that acts through the inhibition of hepatic AMPD2 activity, which is triggered by the gut microbiota.

Acknowledgements

This project was supported by the National Key R&D Program of China (No. 2022YFA0806400), the CAMS Innovation Fund for Medical Sciences (CIFMS; Nos. 2024-I2M-ZH-012 and 2023-I2M-2-006, China), National Natural Science Foundation of China (Nos. 82173888 and 81973290), and Beijing Key Laboratory of Key Technologies for Preclinical Research and Development of Innovative Drugs in Pharmacokinetics and Pharmacodynamics. We would like to thank Shimadzu (China) Co., Ltd., for technological support.

Author contributions

Yan Wang and Jiandong Jiang: conceptualization and methodology. Libin Pan, Ru Feng, Jiachun Hu, Yan Wang: Original draft preparation, writing, review, and editing. Jie Fu, Mengliang Ye: Investigation. Libin Pan, Jiachun Hu, Ru Feng, Hang Yu, Hui Xu, Zhengwei Zhang, Xinyu Yang, Jianye Song, Haojian Zhang, Jinyue Lu, Zhao Zhai, Jingyue Wang, Yi Zhao, and Hengtong Zuo: Validation. Linbin Pan, Ru Feng, Jiachun Hu, Qian Tong, and Yan Wang: Formal analysis. Yan Wang, Jiandong Jiang: Supervision.

Conflicts of interest

Jiandong Jiang, Yan Wang, and Linbin Pan have a patent related to this work (CN201810788495.7). All other authors declare no competing interests.

Supporting information

Supporting information to this article can be found online at <https://doi.org/10.1016/j.apsb.2025.08.009>.

References

- Major TJ, Dalbeth N, Stahl EA, Merriman TR. An update on the genetics of hyperuricaemia and gout. *Nat Rev Rheumatol* 2018;**14**:341–53.
- Liu R, Han C, Wu D, Xia X, Gu J, Guan H, et al. Prevalence of hyperuricemia and gout in Mainland China from 2000 to 2014: a systematic review and meta-analysis. *Biomed Res Int* 2015;**2015**:762820.
- Dalbeth N, Gosling AL, Gaffo A, Abhishek A. Gout. *Lancet* 2021;**397**:1843–55.
- Kasahara K, Kerby RL, Zhang Q, Pradhan M, Mehrabian M, Lusic AJ, et al. Gut bacterial metabolism contributes to host global purine homeostasis. *Cell Host Microbe* 2023;**31**:1038–53.
- DeBosch BJ, Kluth O, Fujiwara H, Schürmann A, Moley K. Early-onset metabolic syndrome in mice lacking the intestinal uric acid transporter SLC2A9. *Nat Commun* 2014;**5**:4642.
- Fan S, Zhang P, Wang AY, Wang X, Wang L, Li G, et al. Hyperuricemia and its related histopathological features on renal biopsy. *BMC Nephrol* 2019;**20**:95.
- White WB, Saag KG, Becker MA, Borer JS, Gorelick PB, Whelton A, et al. Cardiovascular safety of febuxostat or allopurinol in patients with gout. *N Engl J Med* 2018;**378**:1200–10.
- Xing SC, Meng DM, Chen Y, Jiang G, Liu XS, Li N, et al. Study on the diversity of *Bacteroides* and *Clostridium* in patients with primary gout. *Cell Biochem Biophys* 2015;**71**:707–15.
- Shao T, Shao L, Li H, Xie Z, He Z, Wen C. Combined signature of the fecal microbiome and metabolome in patients with gout. *Front Microbiol* 2017;**8**:268.
- Wang J, Chen Y, Zhong H, Chen F, Regenstein J, Hu X, et al. The gut microbiota as a target to control hyperuricemia pathogenesis: potential mechanisms and therapeutic strategies. *Crit Rev Food Sci Nutr* 2022;**62**:3979–89.
- Wang Z, Li Y, Liao W, Huang J, Liu Y, Li Z, et al. Gut microbiota remodeling: a promising therapeutic strategy to confront hyperuricemia and gout. *Front Cell Infect Microbiol* 2022;**12**:935723.
- Tong S, Zhang P, Cheng Q, Chen M, Chen X, Wang Z, et al. The role of gut microbiota in gout: is gut microbiota a potential target for gout treatment. *Front Cell Infect Microbiol* 2022;**12**:1051682.
- Kong W, Wei J, Abidi P, Lin M, Inaba S, Li C, et al. Berberine is a novel cholesterol-lowering drug working through a unique mechanism distinct from statins. *Nat Med* 2004;**10**:1344–51.
- Ma SR, Tong Q, Lin Y, Pan LB, Fu J, Peng R, et al. Berberine treats atherosclerosis via a vitamine-like effect down-regulating Choline–TMA–TMAO production pathway in gut microbiota. *Signal Transduct Targeted Ther* 2022;**7**:207.
- Chang W, Chen L, Hatch GM. Berberine as a therapy for type 2 diabetes and its complications: from mechanism of action to clinical studies. *Biochem Cell Biol* 2015;**93**:479–86.
- Pan L, Yu H, Fu J, Hu J, Xu H, Zhang Z, et al. Berberine ameliorates chronic kidney disease through inhibiting the production of gut-derived uremic toxins in the gut microbiota. *Acta Pharm Sin B* 2023;**13**:1537–53.
- Wang Y, Tong Q, Ma SR, Zhao ZX, Pan LB, Cong L, et al. Oral berberine improves brain dopa/dopamine levels to ameliorate Parkinson's disease by regulating gut microbiota. *Signal Transduct Targeted Ther* 2021;**6**:77.
- Lu Z, He B, Chen Z, Yan M, Wu L. Anti-inflammatory activity of berberine in non-alcoholic fatty liver disease via the Angptl2 pathway. *BMC Immunol* 2020;**21**:28.
- Wang Y, Shou JW, Li XY, Zhao ZX, Fu J, He CY, et al. Berberine-induced bioactive metabolites of the gut microbiota improve energy metabolism. *Metabolism* 2017;**70**:72–84.
- Yao Y, Yan L, Chen H, Wu N, Wang W, Wang D. *Cyclocarya paliurus* polysaccharides alleviate type 2 diabetic symptoms by modulating gut microbiota and short-chain fatty acids. *Phytomedicine* 2020;**77**:153268.
- Macy JM, Ljungdahl LG, Gottschalk G. Pathway of succinate and propionate formation in *Bacteroides fragilis*. *J Bacteriol* 1978;**134**:84–91.
- Van Der Meulen R, Makras L, Verbrugge K, Adriany T, De Vuyst L. *In vitro* kinetic analysis of oligofructose consumption by *Bacteroides* and *Bifidobacterium* spp. indicates different degradation mechanisms. *Appl Environ Microbiol* 2006;**72**:1006–12.
- Robertson AM, Glucina PG. Fructose 6-phosphate phosphorylation in *Bacteroides* species. *J Bacteriol* 1982;**150**:1056–60.
- Oh SF, Praveena T, Song H, Yoo JS, Jung DJ, Erturk-Hasdemir D, et al. Host immunomodulatory lipids created by symbionts from dietary amino acids. *Nature* 2021;**600**:302–7.
- Andres-Hernando A, Cicerchi C, Kuwabara M, Orlicky DJ, Sanchez-Lozada LG, Nakagawa T, et al. Umami-induced obesity and metabolic syndrome is mediated by nucleotide degradation and uric acid generation. *Nat Metab* 2021;**3**:1189–201.
- Lanaspa MA, Epperson LE, Li N, Cicerchi C, Garcia GE, Roncal-Jimenez CA, et al. Opposing activity changes in AMP deaminase and AMP-activated protein kinase in the hibernating ground squirrel. *PLoS One* 2015;**10**:e0123509.
- van den Berghe G, Bronfman M, Vanneste R, Hers HG. The mechanism of adenosine triphosphate depletion in the liver after a load of fructose. A kinetic study of liver adenylate deaminase. *Biochem J* 1977;**162**:601–9.
- Cicerchi C, Li N, Kratzer J, Garcia G, Roncal-Jimenez CA, Tanabe K, et al. Uric acid-dependent inhibition of AMP kinase induces hepatic glucose production in diabetes and starvation: evolutionary implications of the uricase loss in hominids. *FASEB J* 2014;**28**:3339–50.
- Tan XS, Ma JY, Feng R, Ma C, Chen WJ, Sun YP, et al. Tissue distribution of berberine and its metabolites after oral administration in rats. *PLoS One* 2013;**8**:e77969.
- Tang WHW, Wang Z, Kennedy DJ, Wu Y, Buffa JA, Agatista-Boyle B, et al. Gut microbiota-dependent trimethylamine *N*-oxide (TMAO) pathway contributes to both development of renal insufficiency and mortality risk in chronic kidney disease. *Circ Res* 2015;**116**:448–55.
- Chen CH, Chen CB, Chang CJ, Lin YJ, Wang CW, Chi CC, et al. Hypersensitivity and cardiovascular risks related to allopurinol and febuxostat therapy in Asians: a population-based cohort study and meta-analysis. *Clin Pharmacol Ther* 2019;**106**:391–401.
- Yin H, Liu N, Chen J. The role of the intestine in the development of hyperuricemia. *Front Immunol* 2022;**13**:845684.
- Méndez-Salazar EO, Martínez-Nava GA. Uric acid extrarenal excretion: the gut microbiome as an evident yet understated factor in gout development. *Rheumatol Int* 2022;**42**:403–12.
- Iwadata Y, Kato J. Identification of a formate-dependent uric acid degradation pathway in *Escherichia coli*. *J Bacteriol* 2019;**201**:e00573-18.
- Zhang H, Wei J, Xue R, Wu JD, Zhao W, Wang ZZ, et al. Berberine lowers blood glucose in type 2 diabetes mellitus patients through increasing insulin receptor expression. *Metabolism* 2010;**59**:285–92.
- Wang F, Li S, Feng H, Yang Y, Xiao B, Chen D. An enhanced sensitivity and cleanup strategy for the nontargeted screening and targeted determination of pesticides in tea using modified dispersive solid-phase extraction and cold-induced acetonitrile aqueous two-phase systems coupled with liquid chromatography–high resolution mass spectrometry. *Food Chem* 2019;**275**:530–8.
- Feng R, Shou JW, Zhao ZX, He CY, Ma C, Huang M, et al. Transforming berberine into its intestine-absorbable form by the gut microbiota. *Sci Rep* 2015;**5**:12155.
- Wang Y, Tong Q, Shou JW, Zhao ZX, Li XY, Zhang XF, et al. Gut microbiota-mediated personalized treatment of hyperlipidemia using berberine. *Theranostics* 2017;**7**:2443–51.
- Wang L, Ye J. Commentary: gut microbiota reduce the risk of hyperuricemia and gout in the human body. *Acta Pharm Sin B* 2024;**14**:433–5.
- Bode JCH, Zelder O, Rumpelt HJ, Wittkampy U. Depletion of liver adenosine phosphates and metabolic effects of intravenous infusion of fructose or sorbitol in man and in the rat. *Eur J Clin Invest* 1973;**3**:436–41.
- van der Harst P, Bakker SJL, de Boer RA, Wolffenbuttel BHR, Johnson T, Caulfield MJ, et al. Replication of the five novel loci for

- uric acid concentrations and potential mediating mechanisms. *Hum Mol Genet* 2010;**19**:387–95.
42. Akizu N, Cantagrel V, Schroth J, Cai N, Vaux K, McCloskey D, et al. AMPD2 regulates GTP synthesis and is mutated in a potentially treatable neurodegenerative brainstem disorder. *Cell* 2013;**154**:505–17.
 43. Lanaspá MA, Cicerchi C, García G, Li N, Roncal-Jimenez CA, Rivard CJ, et al. Counteracting roles of AMP deaminase and AMP kinase in the development of fatty liver. *PLoS One* 2012;**7**:e48801.
 44. Hudoyo AW, Hirase T, Tandellillin A, Honda M, Shirai M, Cheng J, et al. Role of AMPD2 in impaired glucose tolerance induced by high fructose diet. *Mol Genet Metab Rep* 2017;**13**:23–9.
 45. Qin S, Tang H, Li W, Gong Y, Li S, Huang J, et al. AMPK and its activator berberine in the treatment of neurodegenerative diseases. *Curr Pharm Des* 2020;**26**:5054–66.
 46. Han C, Li L, Bai L, Wu Y, Li J, Wang Y, et al. Neurokinin 1 receptor inhibition alleviated mitochondrial dysfunction *via* restoring purine nucleotide cycle disorder driven by substance P in acute pancreatitis. *Acta Pharm Sin B* 2025;**15**:3025–40.
 47. Huart J, Leenders J, Taminiou B, Descy J, Saint-Remy A, Daube G, et al. Gut microbiota and fecal levels of short-chain fatty acids differ upon 24-hour blood pressure levels in men. *Hypertension* 2019;**74**:1005–13.
 48. Hartwich K, Poehlein A, Daniel R. The purine-utilizing bacterium *Clostridium acidurici* 9a: a genome-guided metabolic reconsideration. *PLoS One* 2012;**7**:e51662.
 49. Porter NT, Luis AS, Martens EC. *Bacteroides thetaiotaomicron*. *Trends Microbiol* 2018;**26**:966–7.
 50. Baughn AD, Malamy MH. The strict anaerobe *Bacteroides fragilis* grows in and benefits from nanomolar concentrations of oxygen. *Nature* 2004;**427**:441–4.
 51. Chu H, Khosravi A, Kusumawardhani IP, Kwon AHK, Vasconcelos AC, Cunha LD, et al. Gene–microbiota interactions contribute to the pathogenesis of inflammatory bowel disease. *Science* 2016;**352**:1116–20.
 52. Zhou W, Wu W, Si Z, Liu H, Wang H, Jiang H, et al. The gut microbe *Bacteroides fragilis* ameliorates renal fibrosis in mice. *Nat Commun* 2022;**13**:6081.
 53. Hsiao EY, McBride SW, Hsien S, Sharon G, Hyde ER, McCue T, et al. Microbiota modulate behavioral and physiological abnormalities associated with neurodevelopmental disorders. *Cell* 2013;**155**:1451–63.
 54. Li LZ, Tao SB, Ma L, Fu P. Roles of short-chain fatty acids in kidney diseases. *Chin Med J (Engl)* 2019;**132**:1228–32.
 55. Banerjee A, Herring CA, Chen B, Kim H, Simmons AJ, Southard-Smith AN, et al. Succinate produced by intestinal microbes promotes specification of Tuft cells to suppress ileal inflammation. *Gastroenterology* 2020;**159**:2101–15.